Title: Transparent ultrathin conducting carbon films

Authors: Martin Schreiber, Tarek Lutz, Gareth P. Keeley, Shishir Kumar, Markus Boese, Satheesh Krishnamurthy, Georg S. Duesberg

PII: S0169-4332(10)00429-0
DOI: doi:10.1016/j.apsusc.2010.03.138
Reference: APSUSC 20043

To appear in: *APSUSC*

Received date: 9-1-2010
Revised date: 28-3-2010
Accepted date: 29-3-2010

Please cite this article as: M. Schreiber, T. Lutz, G.P. Keeley, S. Kumar, M. Boese, S. Krishnamurthy, G.S. Duesberg, Transparent ultrathin conducting carbon films, *Applied Surface Science* (2008), doi:10.1016/j.apsusc.2010.03.138

Transparent ultrathin conducting carbon films

Martin Schreiber[1], Tarek Lutz[1], Gareth P. Keeley[1], Shishir Kumar[1,2], Markus Boese[1], Satheesh Krishnamurthy[1], Georg S. Duesberg[1,2,*]

[1] Centre for Research on Adaptive Nanostructures and Nanodevices (CRANN), Trinity College Dublin, Dublin 2, Ireland
[2] School of Chemistry, Trinity College Dublin, Ireland

Abstract

Ultrathin conductive carbon layers (UCCLs) were created by spin coating resists and subsequently converting them to conductive films by pyrolysis. Homogeneous layers as thin as 3nm with nearly atomically smooth surfaces could be obtained. Layer characterization was carried out with the help of atomic force microscopy, profilometry, four-point probe measurements, Raman spectroscopy and ultraviolet-visible spectroscopy. The Raman spectra and high-resolution transmission electron microscopy image indicated that a glassy carbon like material was obtained after pyrolysis. The electrical properties of the UCCL could be controlled over a wide range by varying the pyrolysis temperature. Variation in transmittance with conductivity was investigated for applications as transparent conducting films. It was observed that the layers are continuous down to a thickness below 10 nm, with conductivities of 1.6 x 10^4 S/m, matching the best values observed for pyrolysed carbon films. Further, the chemical stability of the films and their utilization as transparent electrochemical electrodes has been investigated using cyclic voltammetry and electrochemical impedance spectroscopy.

Keywords:

conductive carbon films; transparent films; pyrolysis; glassy carbon; graphene; electrochemical electrodes

Introduction

Conductive, transparent thin films have important applications in displays, organic light-emitting diodes, organic solar cells, bio-compatible electrodes and optoelectronic devices. The most common of transparent and conductive layers is Indium Tin Oxide (ITO), used because of its high transmittance, high conductivity and suitable work function. However, ITO and related compounds are expensive, and they experience variations in properties such as work function, surface morphology, sheet resistance, etc. between samples from different manufacturers and from different batches [1,2]. ITO layers are also brittle, and that makes them unsuitable for flexible electronics. Further, natural Indium resources are limited. Numerous materials have been investigated to replace ITO [3]. Of these, the use of carbon based materials is particularly attractive because carbon is easily available, cheap and inert. Conductive polymer films (like poly-(3,4 ethylenedioxythiophene - PEDOT), carbon nanotube (CNT) films, graphene films and pyrolytic carbon as possible substitutes to ITO have been discussed in the scientific community [4-12].

In this work we present a cheap and scalable approach to generate ultrathin conductive carbon layers (UCCLs) by spin coating photoresists onto substrates and then annealing them in a vacuum tube furnace under forming gas atmosphere. Upon pyrolysis the resist forms a thin conductive carbon layer also known as pyrolysed photoresist films (PPF) [12-18]. The pristine film thickness is

controlled by the spin speed, viscosity of photoresist solution, evaporation rate and diffusivity of solute [19]. It is also known that polymeric materials, like photoresist films, shrink during pyrolysis which involves crosslinking and side-chain elimination from the original polymer [12,17,18]. Pyrolysis in a reducing atmosphere, typically in forming gas, at temperatures of 700 – 1000 °C removes nearly all the solvent, and most heteroatoms resulting in a significant loss of photoresist weight, yielding a conductive carbonaceous system.[20].

We were able to tune the layer thickness below 100 nm by optimizing the spin coating procedure. Homogenous films down to 3 nm were produced with this simple process, almost reaching the limit obtainable from self-assembled monolayers [21]. The different thick films were investigated in terms of their transparency-conductivity relationship. The morphology was analysed by Raman spectroscopy, high-resolution transmission electron microscopy (HRTEM), and atomic force microscopy (AFM). Further, the utilization of the films as transparent electrochemical electrodes was investigated using cyclic voltammetry and electrochemical impedance spectroscopy.

Experimental

Various photoresists, e.g. PMMA, SU8, AZ nLOF 2070, AZ nLOF 4533, ma-N 20401 with polymer backbones were pyrolysed. These materials are designed to be spin-coated onto substrates, then patterned if desired with standard lithographic techniques. The negative photoresist, AZ nLOF 2070 (*MicroChemicals GmbH, Ulm, Germany*), gave the most the reproducible and reliable results to produce UCCL and is understood below, unless otherwise specified. It consists predominantly of Novolac resin, a further analysis to determine the chemical composition was not performed. Quartz substrates (typically 1.5 cm× 1.5 cm) were cleaned with acetone and isopropanol and afterwards dried with compressed air to remove any traces of dirt or grease from the surface. Under cleanroom conditions the photoresist was spin-coated onto the substrates at angular speeds between 1000 - 6000 rpm for 45 s. AZ EBR (*MicroChemicals GmbH, Ulm, Germany*) was used to dilute the initial amount of photoresist (9 – 30 wt%) in order to get thinner films. After spin coating process the back of the quartz samples was cleaned with acetone and isopropanol. These substrates were soft-baked for 60 s at 100 °C. The samples were then annealed in a vacuum tube furnace (*Gero GmbH*) in forming gas atmosphere (90 % N_2, 10 % H_2). Under continuous gas flow, the temperature was increased at the rate of 3 – 4 °C/min to 650 °C-1000 °C and held there for 60 min, and then cooled to room temperature. Quartz glass can tolerate the high temperatures of the pyrolysis process.

Raman spectra were taken with a Jobin-Yvon Labram Raman spectrometer using an excitation wavelength of 633 nm, with a probe size of 2 μm. Typically, five Raman spectra were taken on each sample to confirm homogeneity over the sample area. A FEI Titan high resolution TEM at 80 kV was used to study the structure of the pyrolysed films, after transfer onto a TEM grid. The layer thickness was measured by profilometry (Dektak 6M, Veeco Instruments). A surgical blade was used with sufficient care to create a small groove on the samples in order to expose the quartz substrate. The UCCL thickness was determined from the difference in height of the photoresist and blank quartz. At least three such profiles at different locations, which were separated at least 1 mm, were taken on each film and the average value was calculated to obtain the thickness of the film. The specified accuracy of the instrument was 1 nm, but our experimental errors were limited to 2-3 nm due to noise. Atomic force microscopy (Asylum Research MFP-3D**)** was used to study the film surface morphology, and as a check on thickness measurements of films.

To investigate the transmittance of the UCCLs all spin coated quartz substrates were analyzed with a ultraviolet-visible spectrometer (Varian Cary 6000i) for wavelengths between 400 nm and 800 nm. The resulting values were averaged to determine the transmittance. As a reference a blank quartz substrate was measured in air to calibrate the background spectrum. Four-point probe measurements at room temperature were taken at different locations on each film using a four-point

probe head (*Jandel*) connected to a Keithley 2400 SourceMeter. Ten measurements were taken to ensure the data integrity and the average value was calculated. The samples were also rotated to ensure that there was no anisotropy in the measurement of the films. The sheet resistance of the carbon films was calculated as $R_s = (V/I) \times CF$ where CF is a sheet resistance correction factor that depends on the sample dimensions and the probe tip spacing [22]. When the layer thickness is several orders of magnitude smaller than the measurement probe distance, $\pi/\ln 2$ can be used as CF [23].

A Gamry 600 potentiostat was used to perform cyclic voltammetry and electrochemical impedance spectroscopy, along with a three-electrode configuration. Platinum wire counter electrodes (CHI115) and Ag / AgCl reference electrodes (CHI111) were supplied by IJ Cambria. The carbon films were incorporated into the electrochemical cell by placing the substrates in a custom-made electrode design. A platinum wire was used to make the electrical contact to the films, and a nitrile 'O' ring defined the electrode surface area as a disc (radius 1.5 mm).

Results and discussion

Pyrolysis induces reorganization of polymer films, resulting in reduction in volume due to loss of solvents and heteroatoms. The amount of reduction depends on chemical identity of the polymer and may occur in lateral and/or transverse directions. The latter can be measured by noting the pre- and post-pyrolysis film thicknesses. Table 1 lists the height values for different photoresists before and after annealing. AZ nLOF films shows 5 fold reduction in thickness while thickness of PMMA layers decreases 10 times. The spread in thickness values at macroscopically separated points on the pre- and post-pyrolysis samples was similar. For example for a 525 nm AZ nLOF film the thickness variation was 1% over the whole substrate prior anneal. After pyrolysis it yielded a 105 nm film with 5% thickness variation. For thinner films the inhomogeneity was slightly higher with 20% for 35 nm thick film over a substrate size of 1 cm^2. This shows that the spin-on procedure and pyrolysis process is uniform on macroscopic scale. Interestingly, changes in lateral dimensions of these films were minor.

AFM was used to study the surface morphology and roughness of produced UCCL. The layers were very homogeneous, featureless and showed no evidence of porosity (Fig. 1(a)). The root mean square (rms) roughness of the pyrolyzed surface over a 1 x 1 μm^2 area was as small as 0.2 nm with peaks < 1 nm (Fig. 1(b)). Thus, UCCL produced by pyrolysis have extremely smooth surfaces, are free of any large aggregates, pinholes and cracks as well as high chemical stability (see below), which are key requirements for various applications, e.g. electrodes used in optoelectronic devices. Compared to these properties, ITO has a relatively rough surface and suffer frequent pinholes, which cause contact problems in some device setups [2,24]. CNT films also have a relatively high surface roughness which is a disadvantage of these films [25].

The HRTEM image (Fig. 1(b)) shows a UCCL film after transfer onto a TEM grid. It shows randomly oriented graphitic regions with local ordering besides curved and disordered structures throughout the layers. The regions of crystalline order have dimensions below 5 nm. The crystallites are larger than those seen in amorphous carbons, and are typically seen in glassy carbon [26,27].

Raman spectroscopy is a powerful tool for characterization of carbon material [28,29]. The principal peaks observed in disordered carbon are the *D* and *G* peaks at ~1330 cm^{-1} and ~1580 cm^{-1} respectively. The *D* peak is related to defects and disorder and stems from breathing modes of A_{1g} symmetry in sp^2 bonded carbon systems. This mode only becomes active in the presence of disorder; it's forbidden in perfect graphite. The *G* peak stems from in-plane bond stretching motion of pairs of carbon atoms, in both rings and chains, and has E_{2g} symmetry; this is observed in all sp^2 bonded carbon systems. Strongly disordered materials such as amorphous carbon have stronger and

broader *D* peaks indicating their random and disordered nature. *G* and *D* peak's position, shape and the intensity ratio $I(D)/I(G)$ provide information about the degree of structural order and crystallite size of carbon network in our films (Fig. 2(a)). Our observation show that at pyrolysis temperature of 650 °C, the *D* peak has its maximum intensity at 1343 cm^{-1}, while the *G* peak has its maximum intensity at 1594 cm^{-1}. With increasing temperature the *G* peak narrows and its position shifts to higher wave numbers, reaching 1601 cm^{-1} at a pyrolysis temperature of 1000 °C. Simultaneously the ratio $I(D)/I(G)$ increases from 0.91 to 1.15 shown in Fig. 2(b), with the position of *D* peak remaining almost constant. The increase in the ratio $I(D)/I(G)$ indicates a decrease in average crystallite size [28], even so at higher temperature anneals should lead to higher degree of grapitisation [16, 30]. This increase in the $I(D)/I(G)$ ratio for anneal for temperatures below 1000 °C has been reported before [31] and it has been suggested that the relation of the $I(D)/I(G)$ ratio to crystallite size is not valid here [32]. However, it should be noted that the *D* band only stems from graphitic structures and there for very small graphitic flakes (~2 nm) in their embryonic state the $I(D)/I(G)$ ratio *increases* [29]. The HRTEM image shows crystallites of this dimensions supporting the assumption that until 1000 °C only very small graphitic regions are formed. Thus, Raman spectra and TEM analysis indicate that our layers are similar to glassy carbon with nano-crystalline structure.

The extent of graphitization with temperature can be gauged by changes in resistivity, with larger graphitization leading to lower resistivities. The conductivity values for 100 nm thick AZ nLOF 2070 films pyrolyzed at different temperature are shown in Fig. 3. The conductivity increases dramatically at 800 °C and above. For example, in this work measured films pyrolyzed at 750 °C show a conductivity of 3.9×10^2 S/m and at 850 °C a conductivity of 4.8×10^3 S/m. The average value observed for conductivity was 2.2×10^4 S/m for 1000 °C heat-treatment. This value is comparable to glass-like carbon. For comparison, commercial available Tokai glassy carbon with a film thickness of 1 μm has a conductivity of $(2.0–2.2) \times 10^4$ S/m for 1000 °C heat-treatment. These results are also in agreement with previous reported results for thick, nontransparent films [14,16,32,33]. The conductivity values of UCCL are comparable to what has been reported for CNT or graphene films with the advantage of facile and reproducible production [7].

The transmittance-conductivity relationship of the UCCLs was investigated. In Fig. 4 the optical transmittance for wavelength from 400 to 800 nm with different thicknesses of AZ nLOF 2070 pyrolyzed at 1000 °C are depicted. Additionally a commercially available 100 nm thick ITO film was also measured as a reference. The films had thicknesses of 3, 13 and 20 nm on quartz substrates. The transmittance of these films was nearly constant over the whole spectral region, with a slight increase at longer wavelength. The transmittance increases as the thickness of the coated film decreases. Typically the transmittance varies from ~91 % to ~25 % as the thickness increases from 3 nm to 88 nm which is in the same range of other transparent pyrolyzed photoresists previously reported [34,35].

The electrical characteristics as a function of transmittance/thickness of our AZ nLOF 2070 UCCL pyrolized at 1000 °C were investigated with four-point probe measurements (Fig. 5). The sheet resistance R_S undergoes a slow increase as the film thickness decreases from ~ 85 nm (transmittance = 20 %; R_S = 600 Ω/□) to ~15 nm (transmittance = 73 %; R_S=3440 Ω/□). Below ~ 15 nm, the sheet resistance shows a more dramatic increase as thickness decreases (7 nm; transmittance = 80 %; R_S = 11000 Ω/□). These results show that the transmittance of this material improves as film thickness decreases, while the sheet resistance increases. The conductivity of the films was calculated using the sheet resistance and thickness of the samples. The averaged conductivity for AZ nLOF 2070 UCCLs (7 - 88 nm) was 1.6×10^4 S/m with a standard deviation of 4×10^3 S/m. Our results are close to results recently published for thin pyrolyzed film by Donner *et al*. (35 - 80 nm, 4.2×10^4 S/m; 13 nm ~ 53 % transmittance) [34], Wang *et al*. (30 nm, 2.1×10^4 S/m; 4 nm ~ 55 % transmittance) [25] and Lee *et al*. (4.5 nm, 4×10^3 S/m; 3 - 4 nm

~ 97 % transmittance) [35]. As already mentioned this value also compares well with reported for much thicker, nontransparent films of pyrolysed photoresist [14,16,18].

The electrochemical characterisation of the carbon films was carried out using the ferro / ferricyanide redox probe. The latter is a recognized benchmark in the investigation of carbon electrodes. It is a near-ideal quasi-reversible system, particularly for carbon surfaces. Cyclic voltammetry was performed using a UCCL electrode in 1 mM ferro / ferricyanide solution. Fig. 6 (a) shows a facile redox process at a sweep rate of 100 mV s^{-1}, with well-defined peaks and a small peak separation. The Nicholson method [36] was employed to calculate a standard electrochemical rate constant of 2.5×10^{-3} cm s^{-1} for the test reaction. This value is very similar to the 2.7×10^{-3} cm s^{-1} previously reported using commercially available glassy carbon electrodes [37]. Electrochemical impedance spectroscopy was also used to show the model behavior of UCCL surfaces. An AC signal was applied with 10 mV amplitude. Data were collected at the standard redox potential in the frequency range 10^{-1} to 10^{5} Hz, and the resulting Nyquist plot in Figure 6(b) shows an ideal fit to the Randles equivalent circuit [38]. The combination of the depressed semicircular feature in the high-frequency region with the linear part in the low-frequency region is characteristic of a system exhibiting mixed control between kinetics and diffusion. Similar behavior is observed at commercially available glassy carbon electrodes [37]. This not only shows the potential of UCCL for usage as electrochemical electrodes, but also proves the chemical stability of our films.

Conclusion

The fabrication of ultrathin conductive carbon layers was demonstrated and the conductivity and transmittance of the layers were investigated. Ultra smooth films were produced with a surface roughness less than 0.2 nm. The Raman spectra and High-resolution transmission electron microscopy image indicate a glassy carbon like material obtained after pyrolysis. The averaged conductivity for produced AZ nLOF 2070 UCCL was 1.6×10^{4} S/m with standard deviation of 4×10^{3} S/m. AZ nLOF 2070 UCCL with transmittances up to > 90 % were produced. These results are within the range highest reported values of other thin pyrolyzed photoresists or precursor polymers discussed in recent literature. One advantage of using the described procedure for device fabrication is the reproducibility of the material due to the high quality of the precursor polymers. Other properties like biocompatibility, chemical inertness, mechanical stability and high density of UCCL are interesting for a number of applications. Using the standard ferro / ferricyanide redox probe, the UCCL surfaces were shown to exhibit electrochemical behaviour typical of commercially available glassy carbon. This novel fabrication technique is a major step to fabricate all carbon electrodes and nanodevices for applications in electrochemistry, bio-sensors and energy conversion.

Acknowledgement

This work was supported by Science Foundation Ireland under the UREKA and the CSET program. TL acknowledges EU founding under the Marie Curie scheme.

References

[1] A.B. Djurisic, C.Y. Kwong, *The Influence of the Electrode Choice on the Performance of Organic Solar Cells*, in: S.-S. Sun, N.S. Sariciftci (Eds.), Organic photovoltaics: mechanismus, materials and devices, Taylor & Francis Ltd., Boca Raton, 2005, pp. 453-477.

[2] B.Zeysing, B. Weßling, *The Dispersion Approach for Buffer Layers and for the Active Light Absorption Layer*, in: C. Brabec, U. Scherf, V. Dyakonov (Eds.), Organic Photovoltaics: Materials, Device Physics, and Manufacturing Technologies, Wiley-VCH, Weinheim, 2008, pp. 243-258.

[3] T. Minami, T. Miyata, *Present status and future prospects for development of non- or reduced-indium transparent conducting oxide thin films*, Thin Solid Films 517 (2008), 1474-1477.

[4] A.C. Arias, M. Granstöm, K. Petritsch, R.H. Friend, O*rganic Photodiodes using Polymeric Anodes*, Synth. Met. 102 (1999), 953- 954.

[5] M. Kaempgen, G. S. Duesberg, S. Roth, *Transparent carbon nanotube coatings,* Applied Surface Science, 252, (2005) 425-429.

[6] M.H. Al-Saleh, U. Sundararaj, *A review of vapor grown carbon nanofiber/polymer conductive composites*, Carbon 49 (2009), 2-22.

[7] L. Hu, D.S. Hecht, G. Grüner, *Infrared transparent carbon nanotube thin films,* Appl. Phys. Lett. 94 (2009), 081103 (3p).

[8] H-Z Geng, K.K. Kim, K.P. So, Y.S. Lee, Y. Chang, Y.H. Lee, *Effect of Acid Treatment on Carbon Nanotube-Based Flexible Transparent Conducting Films*, J. Am. Chem. Soc. 129 (2007), 7758-7759.

[9] K.S. Kim, Y. Zhao, H. Jang, S.Y. Lee, J.M. Kim, K.S. Kim, J-H Ahn, P. Kim, J-Y Choi, B.H. Hong, *Large-scale patern growth of graphene films for stretchable transparent electrodes*, Nature 457 (2009), 706-710.

[10] A. Vollmer, X.L. Feng, X. Wang, L.J. Zhi, K. Müllen, N. Koch, J.P. Rabe, *Electronic and structural properties of graphene-based transparent and conductive thin film electrodes*, Appl. Phys. A: Mater. Sci. Process. 94 (2009), 1-4.

[11] S. De, P.J. King, M. Lotya, A. O'Neill, E.M. Doherty, Y. Hernandez, G.S. Duesberg, J. Coleman, *Flexible, Transparent, Conducting Films of Randomly Stacked Graphene from Surfactant-Stabilized, Oxide-Free Graphene Dispersions*, Small (2009), 1-7, in press.

[12] R. L. McCreery, *Advanced Carbon electrode Materials for Molecular Electrochemistry*, Chem. Rev. 108 (2008), 2646-2687.

[13] J. Kim, X. Song, K. Kinoshita, M. Madou, R. White, *Electrochemical Studies of Carbon Films from Pyrolyzed Photoresist*, J. Electrochem. Soc. 145 (1998), 2314-2319.

[14] S. Ranganathan, R. McCreery, S.M. Majji, M. Madou, P*hotoresist-Derived Carbon for Microelectromechanical Systems and Electrochemical Applications*, J. Electrochem. Soc. 147 (2000), 277-282.

[15] S. Ranganathan, R. McCreery, *Electroanalytical Performance of Carbon Films with Near-Atomic Flatness*, Anal. Chem. 73 (2001), 893-900.

[16] R.Kostecki, B.Schnyder, D.Alliata, X.Song, K.Kinoshita, R.Kötz, *Surface studies of carbon films from pyrolyzed photoresist*, Thin Solid Films 396 (2001), 36-43.

[17] A. Singh, J. Jayaram, M. Madou, S. Akbar, P*yrolysis of Negative Photoresists to Fabricate Carbon Structures for Microelectromechanical Systems and Electrochemical Applications*, J. Electrochem. Soc. 149 (2002), 78-83.

[18] B. Y. Park, L. Taherabadi, C. Wang, J. Zoval, M.J. Madou, *Electrical Properties and Shrinkage of Carbonized Photoresist Films and the Implications for Carbon Microelectromechanical Systems Devices in Conductive Media*, J. Electrochem. Soc. 152 (2005), 136-143.

[19] K. Norrman, A. Ghanbari-Siahkali, N. B. Larsen, *Studies of spin-coated polymer films,* Annu. Rep. Prog. Chem., Sect. C, 101, 174-201 (2005), 174-201.

[20] O.J.A. Schueller, S.T. Brittain, G. M. Whitesides, *Fabrication of glassy carbon microstructures by soft lithography*, Sens. Actuators, A 72 (1999), 125-139.

[21] A. Turchanin, A. Beyer, C.T. Nottbohm, X. Zhang, R. Stosch, A. Sologubenko, J. Mayer, P. Hinze, T. Weimann, A. Gölzhäuser, *One Nanometer Thin Carbon Nanosheets with Tunable Conductivity and Stiffness*, Adv. Mater. 21 (2009), 1233-1237

[22] Y. Sun, O. Ehrmann, J. Wolf, H. Reichl, *The correction factors and their new curve for the measurement of sheet resistance of a square sample with a square four-point probe*, Rev. Sci. Instrum. 63 (1992), 3752-3756.

[23] I. Ruge, M. Mader, *Halbleiter-Technologie*. third ed., Springer, Berlin, 1991.

[24] S. Gardonio, L. Gregoratti, D. Scaini, C. Castellarin-Cudia, P. Dudin, C*haracterization of indium tin oxide surfaces after KOH and HCL treatments*, Org. Electron. 9 (2008), 253-261.

[25] X. Wang, L. Zhi, N. Tsao, Z. Tomovic, J. Li, K. Müllen, *Transparent Carbon Films as Electrodes in Organic Solar Cells*, Angew. Chem., Int. Ed. 47 (2008), 2990-2992.

[26] G.M. Jenkins, K. Kawamura, *Polymeric Carbons – carbon fiber, glass and char*, first ed., Cambridge University Press, Cambridge, 1976.

[27] P.J.F. Harris, *New Perspectives on the Structure of Graphitic Carbons*, Crit. Rev. Solid State Mater. Sci. 30 (2005), 235-253.

[28] F. Tuinstra, J.L. Koenig, *Raman Spectrum of Graphite, J. Chem. Phys.* 53 (1970), 1126-1130.

[29] A.C. Ferrari, J. Robertson, *Resonant Raman spectroscopy of disordered, amorphous, and diamondlike carbon*, Phys. Rev. B: Condens. Matter Mater. Phys. 64 (2001), 1-13.

[30] X. Wang, G. M. Zhang, Y. L. Zhang, F. Y. Li, R. C. Yu, C. Q. Jin, G. T. Zou, *Graphitization of glassy carbon prepared under high temperatures and high pressures,* Carbon, 41(2003), 188-191.

[31] M.R. Baldan, E.C. Almeida, A.F. Azevedo, E.S. Gonçalves, M.C. Rezende, N.G. Ferreira, *Raman validity for crystallite size L_a determination on reticulated vitreous carbon with different graphitization index,* Applied Surface Science, 254 (2007), 600-603.

[32] T-H Ko, W-S Kuo, Y-H Chang, *Raman Study of the Microstructure Changes of Phenolic Resin during Pyrolysis*, Polym. Compos. 21 (2000), 745-750.

[33] A. Singh, J. Jayaram, M. Madou, S. Akbar, P*yrolysis of Negative Photoresists to Fabricate Carbon Structures for Microelectromechanical Systems and Electrochemical Applications*, J. Electrochem. Soc. 149 (2002), 78-83.

[34] S. Donner, H.-W. Li, E.S. Young, M.D. Porter, *Fabrication of Optically Transparent Carbon Electrodes by the Pyrolysis of Photoresist Films: Approach to Single-Molecule Spectroelectrochemistry*, Anal. Chem. 78 (2006), 2816-2822.

[35] H. Lee, R. Rajagopalan, J. Robinson, C.G. Pantano, *Processing and Characterization of Ultrathin Carbon Coatings on Glass*, ACS Appl. Mater. Interfaces 1 (2009), 927-933.

[36] R.S. Nicholson, *Theory and Application of Cyclic Voltammetry for Measurement of Electrode Reaction Kinetics*, Anal. Chem. 37 (1965), 1351-1355.

[37] M.E.G. Lyons, G.P. Keeley, *The Redox Behaviour of Randomly Dispersed Single-Walled Carbon Nanotubes both in the Absence and in the Presence of Adsorbed Glucose Oxidase*, *Sensors* 6 (2006), 1791-1826.

[38] J.E.B. Randles, *Kinetics of rapid electrode reaction*, Disc. Faraday Soc. 1 (1947), 11-19.

Figure captions

Fig. 1. (a) AFM topographical image showing roughness over 1 μm^2 area of a thin pyrolyzed AZ nLOF 2070 film. The highest (white) and lowest (black) points are respectively 1 nm above and 1 nm below the mean height. A height section along the red line is shown below. (b) HRTEM image of a UCCL, showing regions of graphitic ordering (scalebar corresponds to 5 nm).

Fig. 2. Raman spectra **(a)** of 100 nm AZ nLOF 2070 carbon films as a function of pyrolysis temperatures and **(b)** intensity ratio of I(D)/I(G) as a function of the annealing temperature .

Fig. 3. Dependence of conductivity on the pyrolysis temperature of 100 nm thick AZ nLOF 2070 UCCLs. The deviation in each conductivity datapoint is below 3% of the actual value.

Fig. 4. Optical transmittance of 100 nm ITO and AZ nLOF 2070 UCCL pyrolyzed at 1000 °C of various thicknesses as a function of wavelength.

Fig. 5. Sheet resistance / transmittance data for various AZ nLOF 2070 UCCL pyrolyzed at 1000 °C. Error bars are also included for sheet resistance.

Fig. 6. Cyclic voltammogram **(a)** obtained using a UCCL electrode in 1 mM ferro / ferricyanide in 1 M potassium chloride. A sweep rate of 100 mV s^{-1} was employed. **(b)** Nyquist impedance plot obtained at 0.26 V (*vs*. Ag / AgCl).

Figure 1

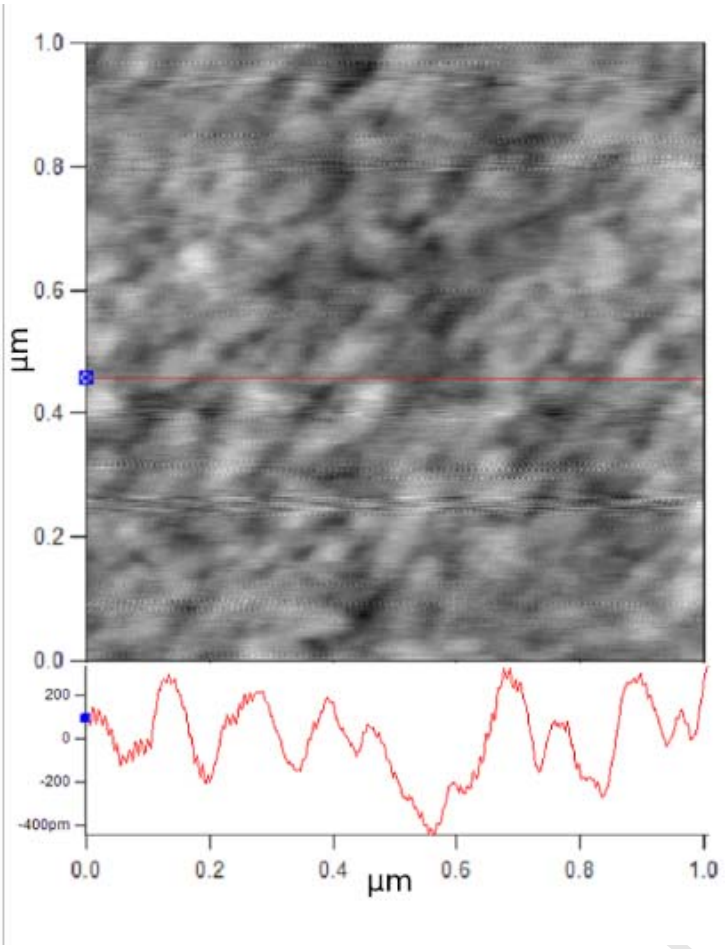

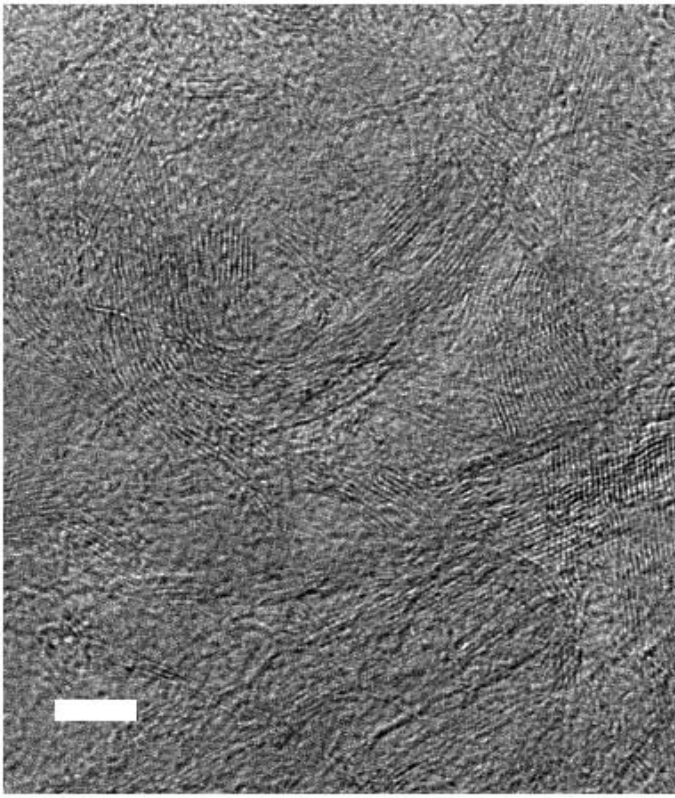

Figure 2

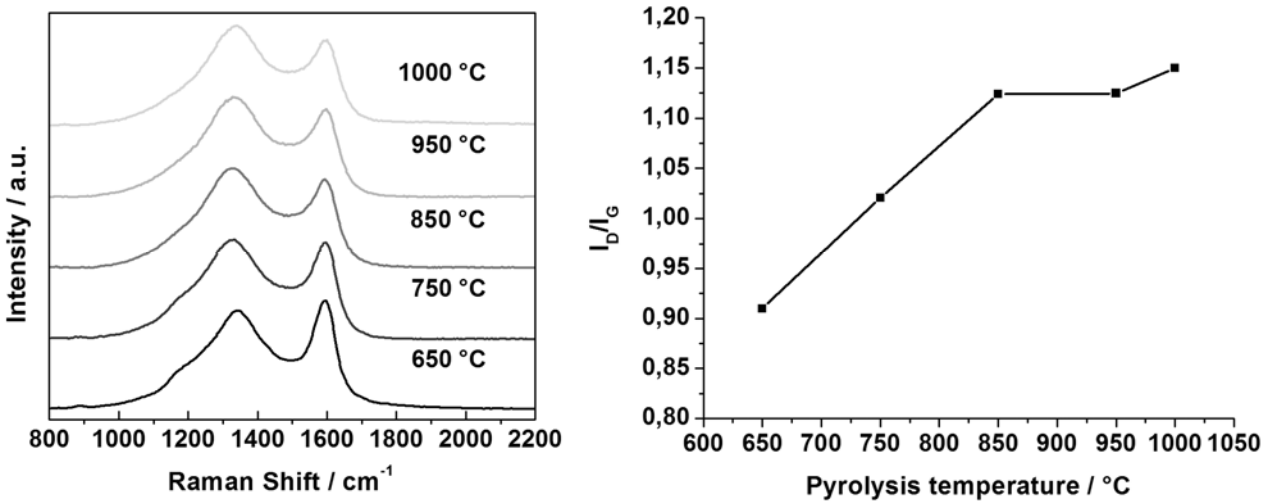

Figure 3

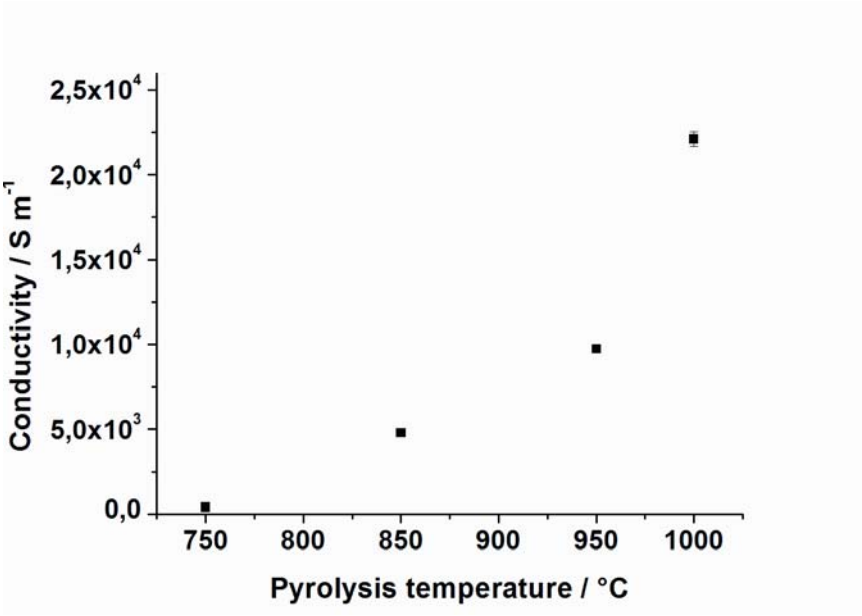

Figure 4

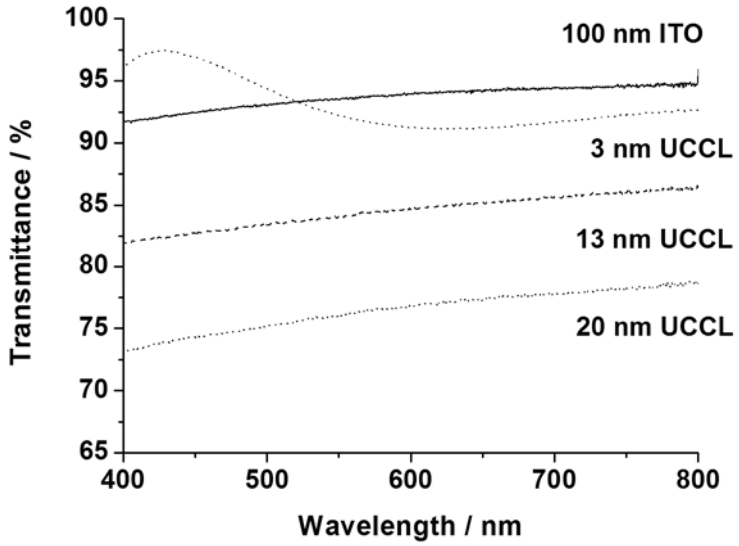

Figure 5

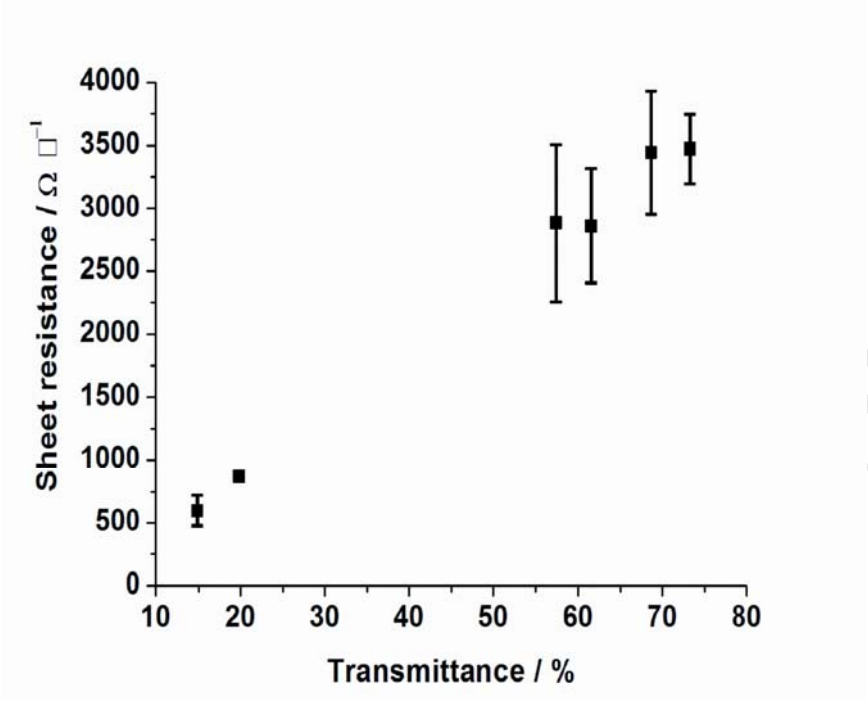

Figure 6

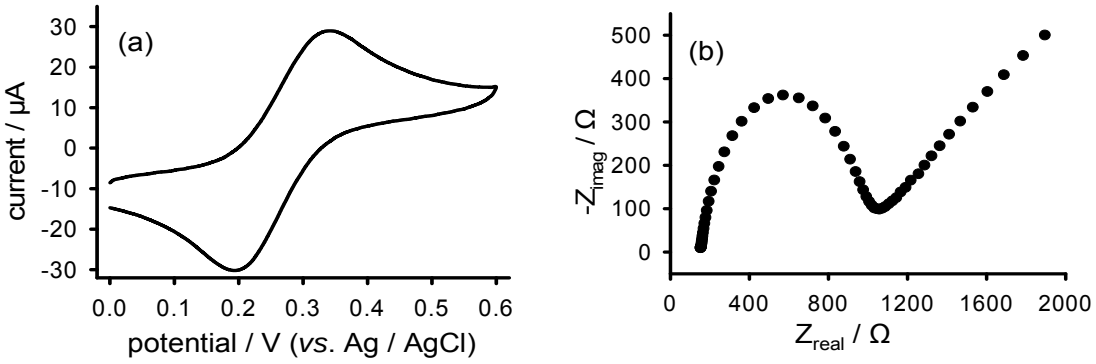

Table captions

Table 1
Summary of resist thickness before and after annealing.

Table 1

Resist	Thickness before anneal [nm]	Thickness after anneal [nm]
nLOF AZ 2070 negative tone resist	518	148
nLOF AZ 2070 (diluted)	35	7
nLOF AZ 4533 positive tone resist	4026	690
ma N 20401 negative tone resist	344	30